Separation Science and Technology
Publication details, including instructions for authors and subscription information:
http://www.informaworld.com/smpp/title~content=t713708471

Numerical Simulation of Elution Chromatography for Separation of H_2-HD-D_2 Mixtures Using a Palladium Particle Bed

Satoshi Fukada[a]
[a] DEPARTMENT OF APPLIED QUANTUM PHYSICS AND NUCLEAR ENGINEERING, GRADUATE SCHOOL OF ENGINEERING, KYUSHU UNIVERSITY, FUKUOKA, JAPAN

Online publication date: 10 December 1999

To cite this Article Fukada, Satoshi(1999) 'Numerical Simulation of Elution Chromatography for Separation of H_2-HD-D_2 Mixtures Using a Palladium Particle Bed', Separation Science and Technology, 34: 14, 2699 — 2721
To link to this Article: DOI: 10.1081/SS-100100800
URL: http://dx.doi.org/10.1081/SS-100100800

SEPARATION SCIENCE AND TECHNOLOGY, **34**(14), pp. 2699–2721, 1999

Numerical Simulation of Elution Chromatography for Separation of H_2–HD–D_2 Mixtures Using a Palladium Particle Bed

SATOSHI FUKADA*
DEPARTMENT OF APPLIED QUANTUM PHYSICS AND NUCLEAR ENGINEERING
GRADUATE SCHOOL OF ENGINEERING
KYUSHU UNIVERSITY
HAKOZAKI, HIGASHI-KU, FUKUOKA, 812-8581, JAPAN

ABSTRACT

Elution chromatography for hydrogen isotope separation is numerically analyzed under conditions where a H_2–HD–D_2 mixture is injected into a palladium particle bed followed by an inert gas purge. When an isotopic mixture of a nearly equal atomic molar fraction of protium and deuterium is developed in the bed with an inert gas purge, effluent concentration bands of each hydrogen species exhibit several characteristics different from ones expected from the Gaussian distribution function. The characteristics are a D_2 band with the highest peak, a HD band with a moderate peak, and a H_2 band drawing a broader or plateau-like curve and having a shoulder around its back end. They are well revealed by the present calculation model. The calculation model is applied to elution chromatography of the six-component hydrogen isotopes using a Pd bed to simulate the isotope separation system of an experimental fusion reactor.

Key Words. Elution chromatography; Palladium; Hydrogen isotope separation; Protium; Deuterium; Tritium; Numerical simulation

INTRODUCTION

Hydrogen isotope separation is a necessary operation for a fuel cycle of an experimental fusion reactor. Gas-chromatographic separation is considered to

* E-mail: s2858tne@mbox.nc.kyushu-u.ac.jp

be one of the most probable methods (1). Palladium or Pd alloys under room temperature and activated alumina under 77 K are the most promising candidates for the packing material.

There are four different chromatographic separation ways using a single-column particle bed: elution, frontal (or breakthrough), displacement, and rotating annular chromatography. Any of them except the last one is a batch process. Continuous separation of gaseous components by the rotating annular chromatography (2) has not been verified successfully by experiment. Previously, some experimental investigations were undertaken for the research and development of the gas-chromatographic separation techniques (3–5). The present author also analytically and experimentally studied the displacement chromatography of a Pd particle bed (6) and the breakthrough chromatography of a yttrium (7) or ZrNi bed (8) using three-component isotopic mixtures (H_2–HD–D_2).

Elution chromatography is numerically studied in the present study. The elution chromatography has been conventionally utilized as the most simplified way to separate a small amount of a gas mixture. Hydrogen isotopes separately emerge from a bed outlet by two steps, i.e., sample gas injection and inert gas purge. There are some analytical approaches such as the plate model (9), the moment analysis (10), and the reverse Laplace transformation by FFT (11). However, they were applied only to linear chromatography and, consequently, are not applicable to the present calculations. The reason is described below.

The shape of elution bands usually appearing in gas chromatography when the system is linear is a Gaussian or Poisson distribution function. A variance or some higher moments of an elution chromatogram are related to the height equivalent to a theoretical plate, HETP (9). However, one should notice that a chromatographic separation system using a metal particle bed is linear only under a very low concentration of deuterium and tritium in hydrogen carrier gas (11, 12). For example, when a mixture of a nearly equal atomic fraction of protium and deuterium is injected into a Pd or Pd alloy particle column, the equilibrium isotherm becomes nonlinear (13). The nonlinearity originates not only from the dependence of the isotope separation factor on concentration but also from the pressure–composition isotherm of the Pd (or its alloy)–hydrogen system (14). Recently, Watanabe et al. (15) presented data of elution chromatography when a mixture of an equal atomic molar fraction of protium and deuterium is injected into a Pd–(8 at%)Pt alloy particle column. Their elution bands are characterized by a comparatively high and narrow D_2 curve, a gradual HD curve, a comparatively lower and wider H_2 curve, and a shoulder appearing at around its back end. As a result, elution chromatograms become far from the Gaussian distribution function. These characteristics can never be explained by any of the above linear analyses. No simulating work has been done

MARCEL DEKKER, INC.
270 Madison Avenue, New York, New York 10016

on the nonlinear Pd–hydrogen isotope separation system. In the present study, nonlinear elution chromatograms are numerically calculated under the condition where an arbitrary mixture of protium and deuterium is injected into a Pd particle column. Calculation results are correlated with respect to effects of the following parameters on elution bands: the mass-transfer capacity coefficients, the isotope separation factor, the sample gas amount and content, and the isotopic equilibrium state of the sample gas.

GOVERNING EQUATIONS FOR NUMERICAL CALCULATION

Pressure–Composition Isotherm

The use of an excess molar chemical potential of atomic hydrogen, μ_H^{excess}, is helpful for describing the pressure–composition isotherm of the Pd–hydrogen (i.e., protium or deuterium) system numerically. Here, μ_H^{excess} is defined in a similar way to Kuji et al. (16) as follows:

$$\mu_H^{excess} = -\Delta\mu_H^0 + \frac{R_g T}{2} \ln\left(\frac{p_{H_2}}{p_0}\right) - R_g T \ln\left(\frac{r}{1-r}\right) \quad (1)$$

The symbols used in the present paper are tabulated in the Nomenclature section. The μ_H^{excess} value is divided into two thermodynamic contributions, i.e., the excess partial molar enthalpy and entropy of dissolved hydrogen, H_H^{excess} and S_H^{excess}. Experimental values of the two thermodynamic quantities were given by previous research (16). We approximated each of them in terms of a fourth-order polynomial of the hydrogen (protium or deuterium) to solid atomic ratio, r;

$$\Delta H_H^{excess} = H_H^{excess} - H_H^{excess}(r = r_0) = \sum_{n=0}^{4} a_{j,n}(r - r_0)^n, \qquad j = \text{H or D} \quad (2)$$

$$\Delta S_H^{excess} = S_H^{excess} - S_H^{excess}(r = r_0) = \sum_{n=0}^{4} b_{j,n}(r - r_0)^n, \qquad j = \text{H or D} \quad (3)$$

where r_0 is an r value at the lower end of the plateau region and depends on temperature.

The plateau pressure of each pure component, $p_{H_2,plat}$ or $p_{D_2,plat}$ (14), is used for the prediction of equilibrium pressure in the thermodynamically unstable region. A set of Eqs. (1) to (3) and $p_{H_2,plat}$ or $p_{D_2,plat}$ can numerically express the entire region of the pressure–composition isotherm of the Pd–protium or –deuterium gas system. Figure 1 shows an example of the equilibrium isotherm of the Pd–protium gas system calculated by Eqs. (1) to (3).

MARCEL DEKKER, INC.
270 Madison Avenue, New York, New York 10016

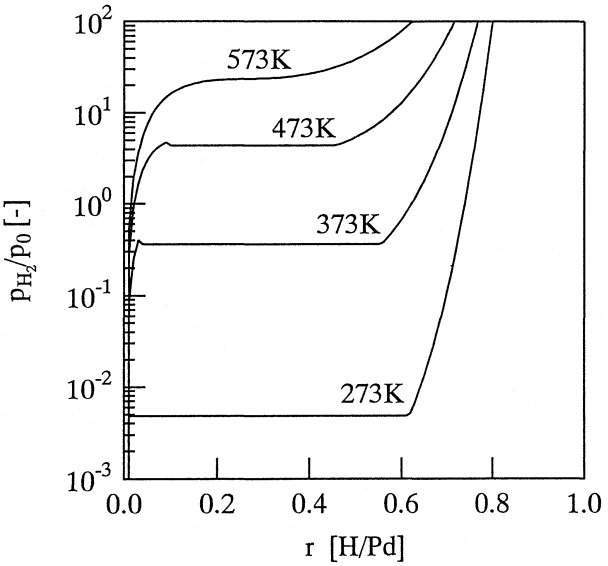

FIG. 1 Equilibrium isotherm of the Pd–hydrogen system.

Isotope Separation Factor and Equilibrium Isotherm of Hydrogen Isotope Mixture

The isotope separation factor between protium and deuterium, $\alpha_{H\text{-}D}$, is defined in terms of the surface concentrations of the gaseous and solid sides, c_{s,H_2}, $c_{s,HD}$, c_{s,D_2}, $q_{s,H}$, and $q_{s,D}$, as follows:

$$\alpha_{H\text{-}D} = \frac{\left(c_{s,D_2} + \frac{1}{2} c_{s,HD}\right) q_{s,H}}{\left(c_{s,H_2} + \frac{1}{2} c_{s,HD}\right) q_{s,D}} \tag{4}$$

The $\alpha_{H\text{-}D}$ is a function of not only temperature but also $q_{s,H}$ and $q_{s,D}$. Its dependency on $q_{s,H}$ and $q_{s,D}$ is well predicted by the ideal solution model (18) as follows:

$$\alpha_{H\text{-}D} = \frac{q_{s,H} + q_{s,D}\alpha_{HD\text{-}D_2}}{(q_{s,H}/\alpha_{H_2\text{-}HD}) + q_{s,D}} \tag{5}$$

The two isotope separation factors in each dilution region of deuterium or protium appearing in Eq. (5), $\alpha_{H_2\text{-}HD}$ and $\alpha_{HD\text{-}D_2}$, are a function of temperature. These constants are related to the equilibrium constant, $K_{H\text{-}D}$, of the isotopic exchange reaction, $H_2 + D_2 = 2HD$, as follows:

$$\alpha_{H_2\text{-}HD} = \alpha^*_{H\text{-}D} \frac{\sqrt{K_{H\text{-}D}}}{2} \tag{6}$$

Marcel Dekker, Inc.
270 Madison Avenue, New York, New York 10016

$$\alpha_{\text{HD-D}_2} = \alpha^*_{\text{H-D}} \frac{2}{\sqrt{K_{\text{H-D}}}} \tag{7}$$

where $\alpha^*_{\text{H-D}}$ is the geometric mean of $\alpha_{\text{H2-HD}}$ and $\alpha_{\text{HD-D2}}$. In other words, $\alpha^*_{\text{H-D}}$ is the isotope separation factor when $c_{\text{s,H}}$ [$= c_{\text{s,H}_2} + (\frac{1}{2})c_{\text{s,HD}}$] = $c_{\text{s,D}}$ [$= c_{\text{s,D}_2} + (1/2)c_{\text{s,HD}}$].

Based on the ideal solution model (7), one gets the equilibrium isotherm of an arbitrary hydrogen isotope mixture consistent with $\alpha_{\text{H-D}}$ defined by Eq. (4). They are expressed by the equations

$$c_{\text{s,H}_2} = \left(\frac{q_{\text{s,H}}}{q_{\text{s,t}}}\right)^2 c^*_{\text{H}_2}(q_{\text{s,t}}) \tag{8}$$

$$c_{\text{s,D}_2} = \left(\frac{q_{\text{s,D}}}{q_{\text{s,t}}}\right)^2 c^*_{\text{D}_2}(q_{\text{s,t}}) \tag{9}$$

$$c_{\text{s,HD}} = (K_{\text{H-D}} c_{\text{s,H}_2} c_{\text{s,D}_2})^{0.5} \tag{10}$$

$$q_{\text{s,t}} = q_{\text{s,H}} + q_{\text{s,D}} \tag{11}$$

in which $c^*_{\text{H}_2}(q_{\text{s,t}})$ and $c^*_{\text{D}_2}(q_{\text{s,t}})$ are molar densities of pure protium and deuterium gas in equilibrium with $q_{\text{s,t}}$, respectively. They are calculated using a relation of $c^*_k = p^*_k/R_gT$ (k = H_2 or D_2) from the equilibrium pressure of the Pd–protium or –deuterium gas system descried in the previous section. The molar fraction is obtained by dividing c_k (k = H_2, HD, D_2) by the total molar density, c_{t} ($= p_{\text{t}}/R_{\text{g}}T$). After introducing Eqs. (5) to (10) into Eq. (4), one can deduce the following relation among $c^*_{\text{H}_2}(q_{\text{s,t}})$, $c^*_{\text{D}_2}(q_{\text{s,t}})$, and $\alpha^*_{\text{H-D}}$:

$$\alpha^*_{\text{H-D}} = \left[\frac{c^*_{\text{D}_2}(q_{\text{s,t}})}{c^*_{\text{H}_2}(q_{\text{s,t}})}\right]^{0.5} = \frac{q_{\text{s,H}} c^{0.5}_{\text{s,D}_2}}{q_{\text{s,D}}\, c^{0.5}_{\text{s,H}_2}} \tag{12}$$

Equation (12) means that the ratio of $c^*_{\text{H}_2}(q_{\text{s,t}})$ to $c^*_{\text{D}_2}(q_{\text{s,t}})$ is constant regardless of $q_{\text{s,t}}$ under the assumption of the ideal solution model.

Thus, any equilibrium isotherm of an arbitrary H_2–HD–D_2 mixture can be expressed in terms of the set of $c^*_{\text{H}_2}(q_{\text{s,t}})$ and $\alpha^*_{\text{H-D}}$ or $c^*_{\text{H}_2}(q_{\text{s,t}})$ and $c^*_{\text{D}_2}(q_{\text{s,t}})$. In the present study, I used the set of $c^*_{\text{H}_2}(q_{\text{s,t}})$ and $\alpha^*_{\text{H-D}}$ because more data are available (17, 18).

Material Balance Equation and Hydrogenating Rate Equation

The material balance equation in a particle bed for each molecular species is expressed by the equation

$$\frac{\partial c_k}{\partial t} + \frac{u}{\varepsilon}\frac{\partial c_k}{\partial z} + \frac{j_k}{\varepsilon} = D_{\text{L}}\frac{\partial^2 c_k}{\partial z^2}, \qquad k = \text{H}_2, \text{HD}, \text{D}_2 \tag{13}$$

MARCEL DEKKER, INC.
270 Madison Avenue, New York, New York 10016

The term including the axial dispersion coefficient on the right-hand side of Eq. (13) was neglected in a similar way to our previous research (7). Each molar flux onto Pd particles per unit bed volume, j_k (k = H_2, HD, and D_2), is expressed in terms of two mass-transfer capacity coefficients:

$$j_k = k_{\mathrm{abs},k} a_\mathrm{v} (c_k - c_{\mathrm{s},k}), \qquad k = \mathrm{H_2, HD, D_2} \tag{14}$$

$$j_j = \gamma \frac{\partial q_{\mathrm{m},j}}{\partial t} = \gamma k_{\mathrm{dif},j} a_\mathrm{v} (q_{\mathrm{s},j} - q_{\mathrm{m},j}), \qquad j = \mathrm{H, D} \tag{15}$$

$$j_\mathrm{H} = 2j_{\mathrm{H_2}} + j_\mathrm{HD}, \qquad j_\mathrm{D} = 2j_{\mathrm{D_2}} + j_\mathrm{HD} \tag{16}$$

The right-hand-side term on Eq. (14) is a molar absorption rate of each hydrogen molecular species on solid surfaces per unit bed volume, and the term on the right-hand side of Eq. (15) is a molar diffusion rate of each hydrogen atomic species in the solid phase. The solid-phase mass-transfer capacity coefficient, $k_{\mathrm{dif},j} a_\mathrm{v}$ (j = H, D), relates to the hydrogen diffusion coefficient in the solid particle, $D_{\mathrm{s},j}$ (j = H, D), through a simple relation of $k_{\mathrm{dif},j} a_\mathrm{v} = 15 D_{\mathrm{s},j}/a^2$ if the solid is a spherical particle.

The initial and boundary conditions for the present elution chromatography are as follows:

$$t = -t_0 \qquad q_j = 0 \qquad j = \mathrm{H, D} \tag{17}$$

$$z = 0, -t_0 \le t \le 0 \qquad c_k = c_{0,k} \qquad k = \mathrm{H_2, HD, D_2} \tag{18}$$

$$t \ge 0 \qquad c_k = 0 \qquad k = \mathrm{H_2, HD, D_2} \tag{19}$$

There are kinetic isotope effects among both $k_{\mathrm{dif},j} a_\mathrm{v}$ (j = H, D) and $k_{\mathrm{abs},k} a_\mathrm{v}$ (k = H_2, HD, D_2). The relation of $D_{\mathrm{s,D}}/D_{\mathrm{s,H}} = 0.68 \exp(232/T)$ was used for the evaluation of the isotope effect in $D_{\mathrm{s},j}$ of Pd (19). However, we had no data on the kinetic isotope effect among $k_{\mathrm{abs},k} a_\mathrm{v}$. For convenience in calculating, we substituted a hypothetical value for each $k_{\mathrm{abs},k} a_\mathrm{v}$ (k = H_2, HD, D_2). A wrong evaluation of $k_{\mathrm{abs},k} a_\mathrm{v}$ might lead us to a different result, especially if the rate-controlling step was the hydrogen absorption rate. Therefore, the effect of the isotopic difference among $k_{\mathrm{abs},k} a_\mathrm{v}$ on an elution chromatogram is investigated numerically in detail.

Dimensionless Parameters

It is more convenient to calculate numerical elution chromatograms using dimensionless equations because of the reduction of the number of parameters. The two isotopic differences among $k_{\mathrm{abs},k} a_\mathrm{v}$ (k = H_2, HD, D_2) and $k_{\mathrm{dif},j} a_\mathrm{v}$ (j = H, D) are correlated to their respective nondimensional parameters.

$$\phi_{\mathrm{abs},k} = \frac{k_{\mathrm{abs},k}}{k_{\mathrm{abs,H_2}}}, \qquad k = \mathrm{HD, D_2} \tag{20}$$

$$\phi_{\mathrm{dif,D}} = \frac{k_{\mathrm{dif,D}}}{k_{\mathrm{dif,H}}} \tag{21}$$

The two mass-transfer capacity coefficients are also correlated to the following two nondimensional parameters:

$$\eta = \frac{c_{0,\mathrm{t}} k_{\mathrm{abs,H_2}} a_{\mathrm{v}}}{\gamma k_{\mathrm{dif,H}} a_{\mathrm{v}} q_{0,\mathrm{t}}} \tag{22}$$

$$\zeta_{\mathrm{h}} = \frac{\gamma k_{\mathrm{dif,H}} a_{\mathrm{v}} q_{0,\mathrm{t}} h}{u c_{0,\mathrm{t}}} \tag{23}$$

The concentration of each species in the bed, c_k (k = H_2, HD, D_2), is normalized by the total inlet concentration, $c_{0,\mathrm{t}}$ ($= c_{0,\mathrm{H_2}} + c_{0,\mathrm{HD}} + c_{0,\mathrm{D_2}}$).

The inlet condition is correlated in terms of the following parameters:

$$\phi_0 = \frac{2c_{0,\mathrm{D_2}} + c_{0,\mathrm{HD}}}{2c_{0,\mathrm{H_2}} + c_{0,\mathrm{HD}}} \tag{24}$$

$$\phi^+_{0,\mathrm{D_2}} = \frac{c_{0,\mathrm{D_2}}}{c_{0,\mathrm{H_2}}} \tag{25}$$

$$\phi^+_{0,\mathrm{HD}} = \frac{c_{0,\mathrm{HD}}}{c_{0,\mathrm{H_2}}} \tag{26}$$

When the gas sample is injected into the bed under the isotopic equilibrium state, the relations among ϕ_0, $\phi^+_{0,\mathrm{D_2}}$ and $\phi^+_{0,\mathrm{HD}}$ hold true.

$$\phi^+_{0,\mathrm{D_2}} = \left[\frac{\sqrt{K_{\mathrm{H\text{-}D}}}(\phi_0 - 1) + \sqrt{K_{\mathrm{H\text{-}D}}(\phi_0 - 1)^2 + 16\phi_0}}{4} \right]^2 \tag{27}$$

$$\phi^+_{0,\mathrm{HD}} = \sqrt{K_{\mathrm{H\text{-}D}} \phi^+_{0,\mathrm{D_2}}} \tag{28}$$

When $c_{0,\mathrm{HD}}$ is not present in the inlet gas, the results are $\phi^+_{0,\mathrm{D_2}} = \phi_0$ and $\phi^+_{0,\mathrm{HD}} = 0$.

The sample amount is correlated in terms of the following nondimensional parameter, $m_{0,\mathrm{t}}$:

$$m_{0,\mathrm{t}} = \frac{u t_0 (c_{0,\mathrm{H_2}} + c_{0,\mathrm{HD}} + c_{0,\mathrm{D_2}})}{\gamma h (q_{0,\mathrm{H}} + q_{0,\mathrm{D}})} \tag{29}$$

The dimensionless time appearing in figures in the present paper, τ/ζ_{h} ($= uc_{0,\mathrm{t}}(t - \varepsilon h/u)/\gamma q_{0,\mathrm{t}} h$), has a meaning of dimensionless stoichiometric time. When a Pd bed continues to be supplied with the sample gas of $c_{0,\mathrm{t}}$ ($= c_{0,\mathrm{H_2}} + c_{0,\mathrm{HD}} + c_{0,\mathrm{D_2}}$) until $\tau/\zeta_{\mathrm{h}} = 1$, it is just saturated with the hydrogen isotope mixture. Other nondimensional governing equations are summarized in the Appendix.

MARCEL DEKKER, INC.
270 Madison Avenue, New York, New York 10016

The dimensionless differential equations, Eqs. (A-1) and (A-2), were numerically solved by the predictor–corrector method along characteristic lines (21). The algebraic equations, Eqs. (A-3) to (A-8), were simultaneously solved by the Newton–Raphson method. Calculation was repeatedly carried out until a relative calculation correction became less than 10^{-5}.

NUMERICAL RESULTS AND DISCUSSION

Effect of Sample Amount on Chromatogram

Figures 2(a) to (d) show examples of variations of the elution chromatogram with time for different values of the dimensionless sample amount, $m_{0,t}$. The other dimensionless parameters are constant throughout the figures, and p_t is 101.3 kPa. The total amount of hydrogen injected into the column is one of the most important factors affecting the shape of the elution chromatogram. Characteristics similar to the previous experiment (15) emerge from each band of hydrogen isotopes for larger $m_{0,t}$ as seen in Figs. 2(c) and (d). The characteristics are a D_2 band with the highest peak height, a HD band with a gradual slope, and a similarly gradual (or plateau-like) H_2 band which has a sharp edge around its back end.

When $m_{0,t}$ becomes larger within maximally unity, sufficient operation for separation is imposed on the gas mixture injected, while not sufficient when a small amount of sample is fed. This thought may seem different from our mere intuition judging from linear chromatography; a less amount of sample should result in more separative action in a column of a specified length. A key to answer the question is to understand that two-step separation is proceeding in the Pd bed. This means, displacement by hydrogen isotopes themselves is developed in the bed with an inert gas purge (20). When the sample amount is large, a hydrogen isotope with lower affinity for Pd (deuterium in this case) is displaced by another isotope with higher affinity (protium in this case). The desorption process by inert gas follows this. When $m_{0,t}$ is 0.75, as seen in Fig. 2(d), the nonlinear features are the most remarkable among all the numerical chromatograms. On the other hand, a smaller amount of the sample results in less separative action as seen in Fig. 2(a). The latter is similar to a linear chromatogram, i.e., a Poisson profile.

Profile of Hydrogen Isotope Absorption Amount over Bed

Figures 3(a) to (d) show examples of the longitudinal profile of the absorbed hydrogen isotope amount averaged over a particle at a dimensionless position, z/h, for different dimensionless times, τ/ζ_h. The τ/ζ_h value is the same as the abscissa of Fig. 2, i.e., $uc_{0,t}(t - \varepsilon h/u)/\gamma q_{0,t}h$. The influent conditions are the same as those of Fig. 2(d). In the early stage of the elution pro-

MARCEL DEKKER, INC.
270 Madison Avenue, New York, New York 10016

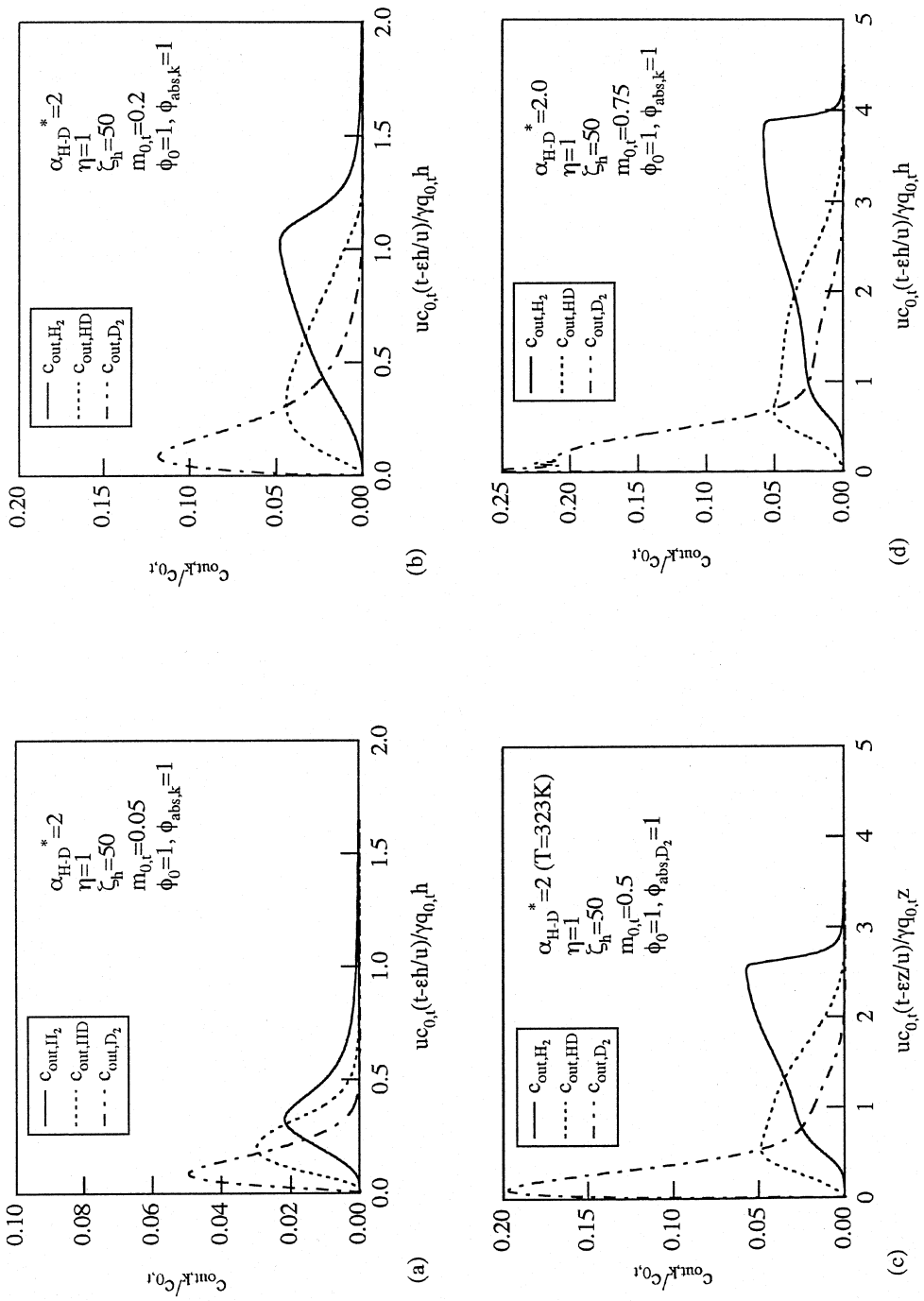

FIG. 2 Variations of hydrogen isotope elution chromatograms with time for different sample amounts (different $m_{0,t}$ values in the dimensionless form).

MARCEL DEKKER, INC.
270 Madison Avenue, New York, New York 10016

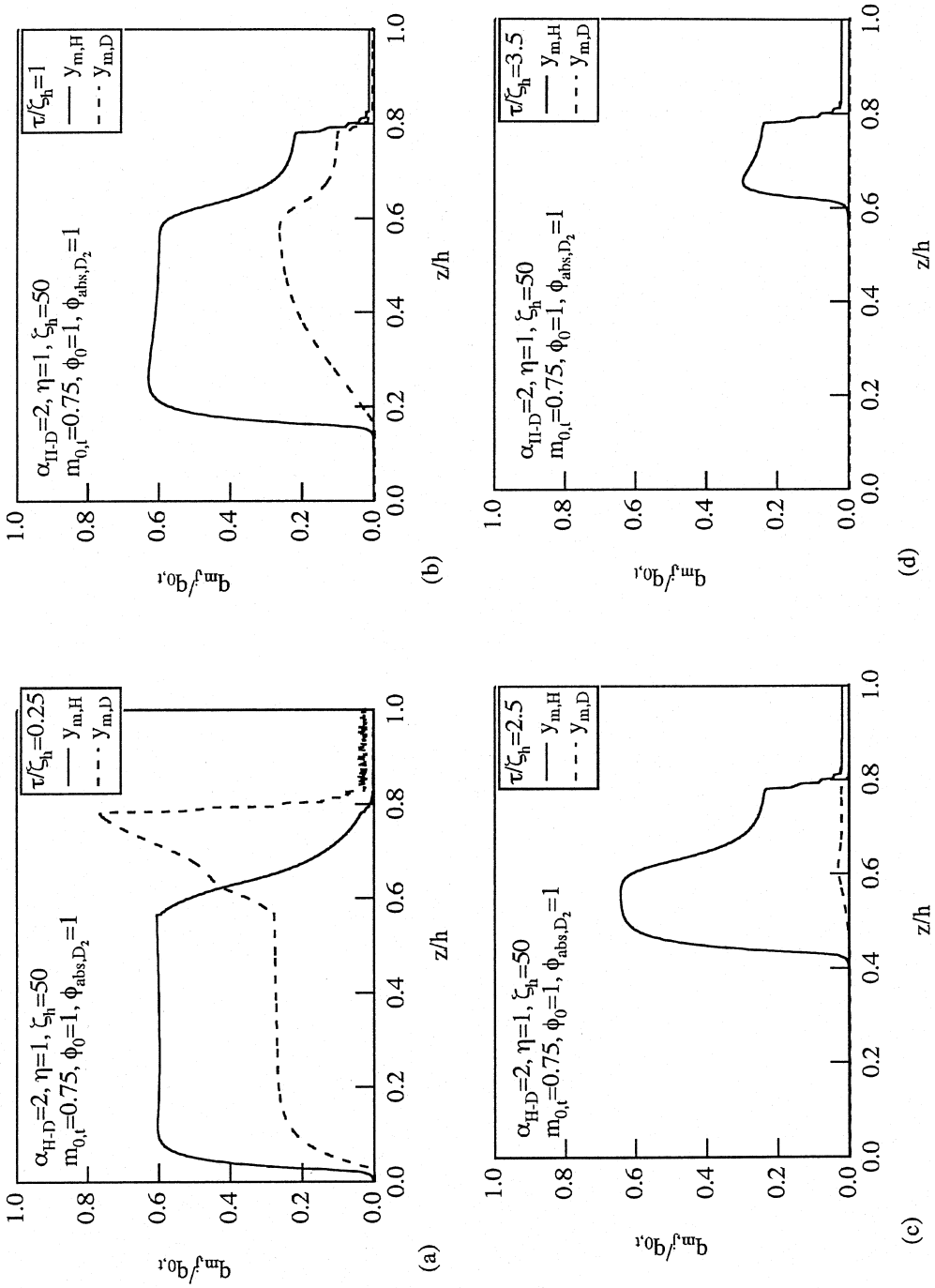

FIG. 3 Profiles of hydrogen isotope absorption amount in Pd bed.

MARCEL DEKKER, INC.
270 Madison Avenue, New York, New York 10016

cess, as seen in Fig. 3(a), the respective profiles can be divided into four regions: a near inlet region of $0 < z/h < 0.1$, a plateau region of $0.1 < z/h < 0.6$, a deuterium-concentrated region of $0.6 < z/h < 0.8$, and a near outlet region of $0.8 < z/h < 1$. Their respective boundaries vary with time.

At $\tau/\zeta_h = 0.25$, both values of $y_{m,H}$ and $y_{m,D}$ on the ordinate are almost flat in the plateau region. The Pd particles in this region are in the lower limit of the hydride phase (the upper limit of the two-phase region) of the Pd–hydrogen system, and the displacement process between protium and deuterium prevails against the desorption process by the cocurrent inert gas. Displaced deuterium atoms are pushed out in the downward direction of the bed. Consequently, the deuterium-concentrated region emerges in $0.6 < z/h < 0.8$ at $\tau/\zeta_h = 0.25$. The particles in the concentrated region are also in the upper limit of the two-phase region. The hydrogen absorption amount is almost unchanged between the deuterium-concentrated region and the plateau region. The Pd particles in the near outlet region are in the solid-solution region. Since the affinity of all the hydrogen isotopes for Pd is much higher than that of inert gas, the front end of the hydride phase located at around $z/h = 0.8$ is very sharp. The migration velocity of the front end is very slow or the boundary almost stands still, so that the hydrogen content of the Pd particles near the outlet is always in the higher limit of the solid-solution region.

As the bed continues to be supplied with the inert gas, the deuterium-concentrated region shrinks. Deuterium is preferentially exhausted from the bed until $\tau/\zeta_h < 1$. Then separation of deuterium is attained at the outlet. Before $\tau/\zeta_h = 2.5$, deuterium is almost completely desorbed from the bed. The slopes of the HD and H_2 elution bands are gradual during $1 < \tau/\zeta_h < 3.5$. This is because the hydrogen content of the Pd particles near the outlet is always in the higher limit of the solid-solution phase during $1 < \tau/\zeta_h < 3.5$. The H_2 band draws a plateau-like curve. When $\tau/\zeta_h = 3.9$, the boundary between the near inlet region and the plateau region comes up with the hydride front end. Then the hydride phase disappears from the Pd particles throughout the bed. A shoulder is observed on the H_2 band at the outlet.

Effect of $\alpha^*_{H\text{-}D}$ on Chromatogram

Figures 4(a) and (b) and Fig. 2(c) illustrate examples of variations of the numerical chromatogram with time for different $\alpha^*_{H\text{-}D}$ values. With lowering temperature, $\alpha^*_{H\text{-}D}$ increases. As expected, a larger $\alpha^*_{H\text{-}D}$ leads to better separation.

An elution time is usually defined by the time when each chromatogram peak passes through the bed outlet. The elution time delays more with lowering temperature. The elution time of each component at 273 K (Fig. 4b) is more than ten times longer than that at 323 K (Fig. 2c). This is because hydrogen is easily desorbed from the bed at elevated temperatures. On the other

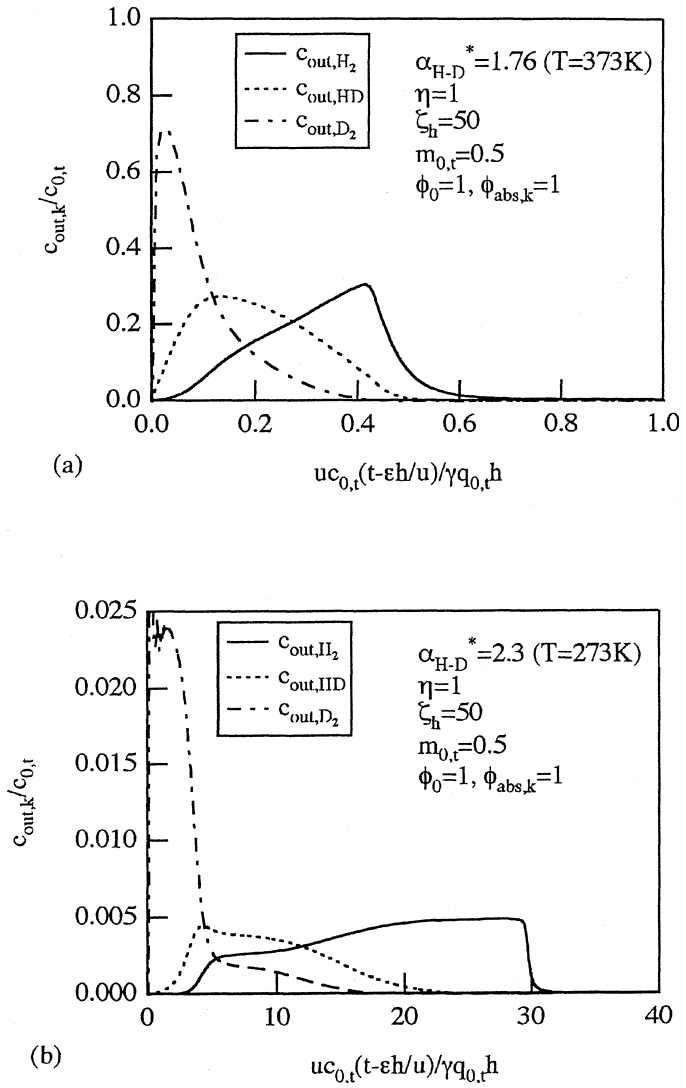

FIG. 4 Variations of hydrogen isotope elution chromatograms with time for different bed temperatures (different $\alpha^{*}_{H\text{-}D}$ values).

hand, the three peaks are less separated when $\alpha^{*}_{H\text{-}D}$ approaches unity as seen in Fig. 4(a). Thus, there is a desirable temperature to operate the Pd bed (around 323 K).

Effect of Mass-Transfer Capacity Coefficients on Elution Chromatogram

Figures 5(a) and (b) and Fig. 2(b) show examples of variations of the numerical chromatogram from the Pd bed with time for different values of η, which is a dimensionless parameter on mass transfer. The other dimensionless

mass-transfer parameter, ζ_h, along with $\alpha^*_{H\text{-}D}$, $m_{0,t}$, ϕ_0, and $\phi_{abs,k}$ (k = H_2, HD, D_2), are constant throughout the figures. An increase in η under constant ζ_h means a decrease in the contribution of the gaseous phase mass-transfer resistance to chromatogram (in other words, an increase in the absorption rate). When η is 10, the characteristics in the three elution bands become more remarkable. On the other hand, as η becomes smaller, the characteristics disappear from the curves.

Figures 6(a) and (b) and Fig. 2(b) show examples of variations of the numerical chromatogram with time for a set of different ζ_h and η values under constant $\zeta_h\eta$ (= 50) throughout the three figures. The constant $\zeta_h\eta$ means the

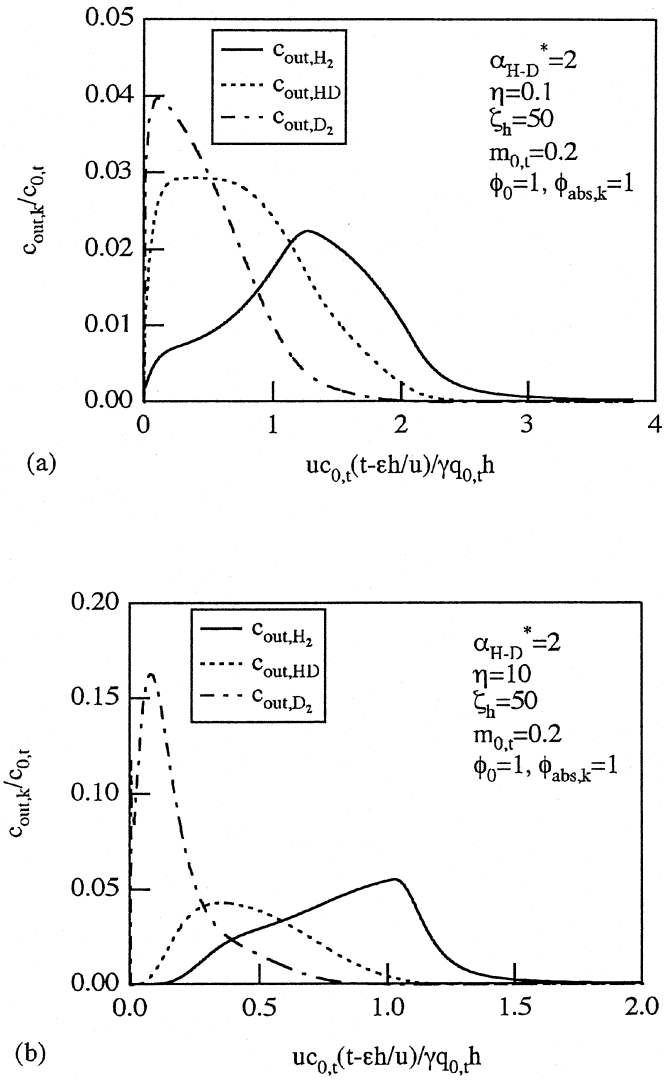

FIG. 5 Variations of hydrogen isotope elution chromatograms with time for different $k_{abs,k}a_v$ values (different η values in the dimensionless form).

MARCEL DEKKER, INC.
270 Madison Avenue, New York, New York 10016

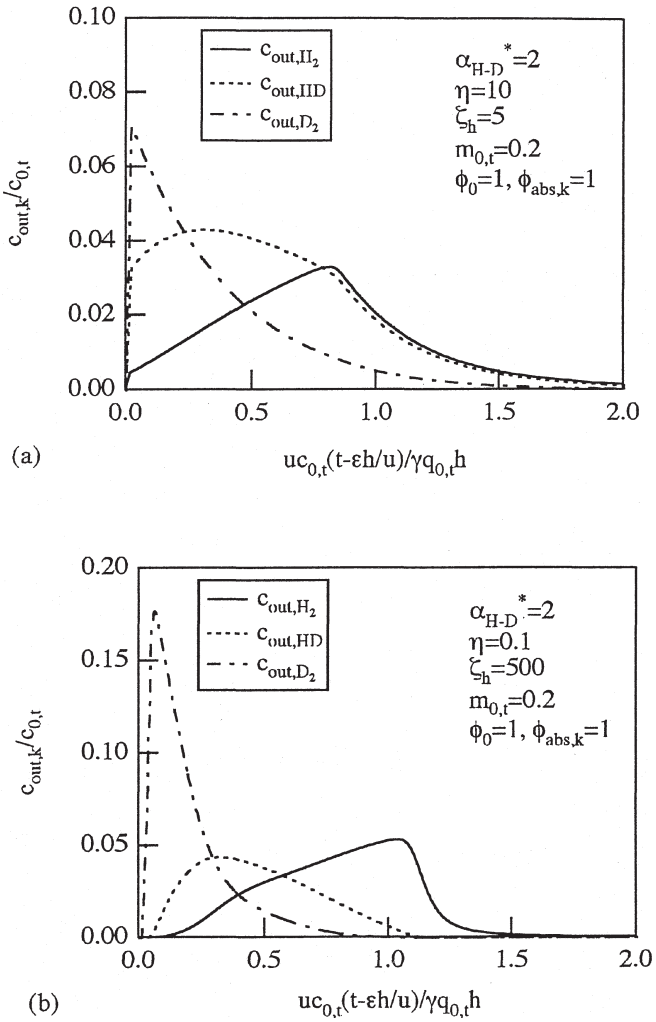

FIG. 6 Variations of hydrogen isotope elution chromatograms with time for different $k_{dif,j}a_v$ values (under the constant $\eta\zeta_h$ value in the dimensionless form).

same $k_{abs,H_2}a_v$ condition. As ζ_h becomes larger under the same $k_{abs,H_2}a_v$, the solid-phase mass-transfer resistance becomes smaller. Then the above characteristics on the nonlinear chromatography become more remarkable in a similar way to changes of η. With a drop of ζ_h, on the other hand, any bands are less separated from each other.

Effect of Isotopic Difference in $k_{abs,k}a_v$ on Chromatogram

Figures 7(a) and (b) and Fig. 2(c) show results of the effect of isotopic differences among $k_{abs,k}a_v$ (k = H_2, HD, D_2) on an elution chromatogram. For convenience, the relation of $k_{abs,HD} = (k_{abs,D_2}k_{abs,H_2})^{0.5}$ is additionally as-

MARCEL DEKKER, INC.
270 Madison Avenue, New York, New York 10016

sumed throughout the present calculations. A much greater or lesser ϕ_{abs,D_2} value than unity means a larger isotopic difference between $k_{abs,H_2}a_v$ and $k_{abs,D_2}a_v$. Judging from many calculations under the present and other conditions, the kinetic isotope effects among $k_{abs,k}a_v$ ($k = H_2$, HD, D_2) affect elution chromatograms less compared with $\alpha^*_{H\text{-}D}$, η, and ζ_h. The degree of the nonlinear characteristics on the elution chromatogram hardly changed regardless of the isotopic differences in $\phi_{dif,j}$ as well as in $\phi_{abs,k}$. This result implicitly means that the nonlinear characteristics originate not from the hydrogenating rate process but from the static difference in the equilibrium condition in Pd among hydrogen isotopes. The latter is quantitatively evaluated by $\alpha^*_{H\text{-}D}$ and the equilibrium isotherm in the present paper.

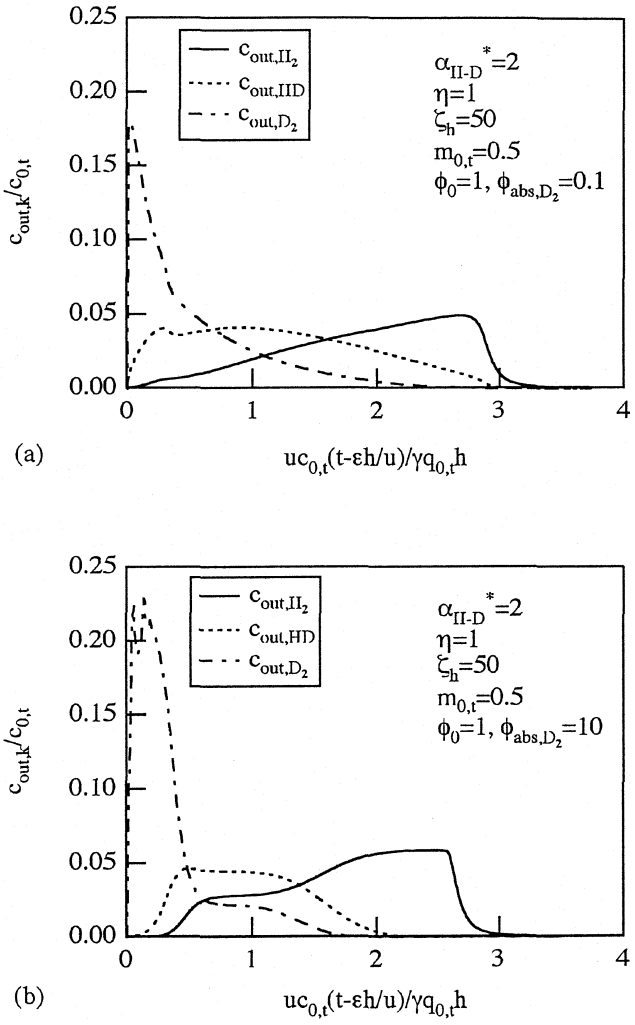

FIG. 7 Variations of hydrogen isotope elution chromatograms with time for different isotope effects of $k_{abs,k}$ (different $\phi_{abs,k}$ values in the dimensionless form).

MARCEL DEKKER, INC.
270 Madison Avenue, New York, New York 10016

Effect of Isotopic Equilibrium State on Elution Chromatogram

All of the previous results shown in Figs. 2 to 7 are calculated under the condition where the supplied gas is in isotopic equilibrium. Figure 8 is calculated under the condition where HD is not present in the inlet gas. Comparison between Fig. 8 and Fig. 5(b) teaches us that the isotopic equilibrium state of the injected gas sample is also an affecting factor. When HD is not present in the inlet gas ($\phi^{+}_{0,HD} = 0$), HD starts being generated immediately after the $H_2 + D_2$ mixture is supplied to the bed. After a short time elapses, the D_2 band is displaced by a mixture of a small amount of HD and a large amount of H_2. Therefore, in that case, insufficient separation is imposed on the D_2 band. On the other hand, when the sample gas is injected under the isotopic equilibrium state, a HD band is formed near the inlet sufficient for separation. Therefore the D_2 band is sufficiently displaced by the HD band. Thereafter, the HD band is displaced by the pure H_2 band. Thus, the isotopic equilibrium condition is preferable for the development of each hydrogen isotope band.

Effect of Sample Content on Elution Chromatogram

Figures 9(a) and (b) and Fig. 2(c) show examples of variations of the elution chromatogram with time for different sample concentrations. The chromatograms in both cases of the deuterium-dominant ($\phi_0 > 1$) and protium-dominant ($\phi_0 < 1$) samples are not satisfactory with respect to complete separation. For the protium-dominant inlet gas as seen in Fig. 9(a), the D_2 band is concealed behind the other bands so that a product with a very high concentration of deuterium cannot be obtained by means of the once-through operation. In other words, the elution chromatography may not be efficient un-

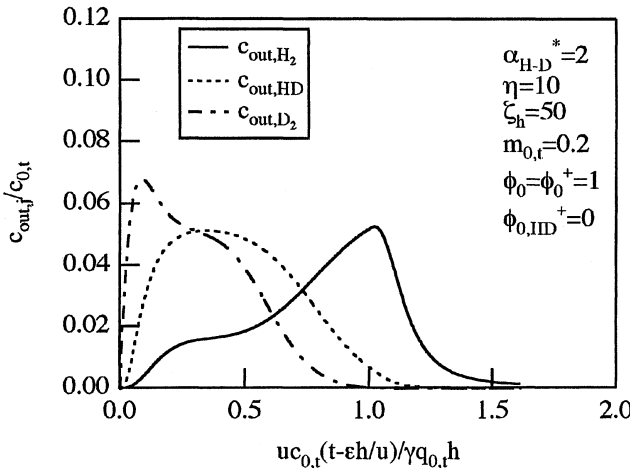

FIG. 8 Elution chromatograms when the isotopic equilibrium is not reached at inlet.

MARCEL DEKKER, INC.
270 Madison Avenue, New York, New York 10016

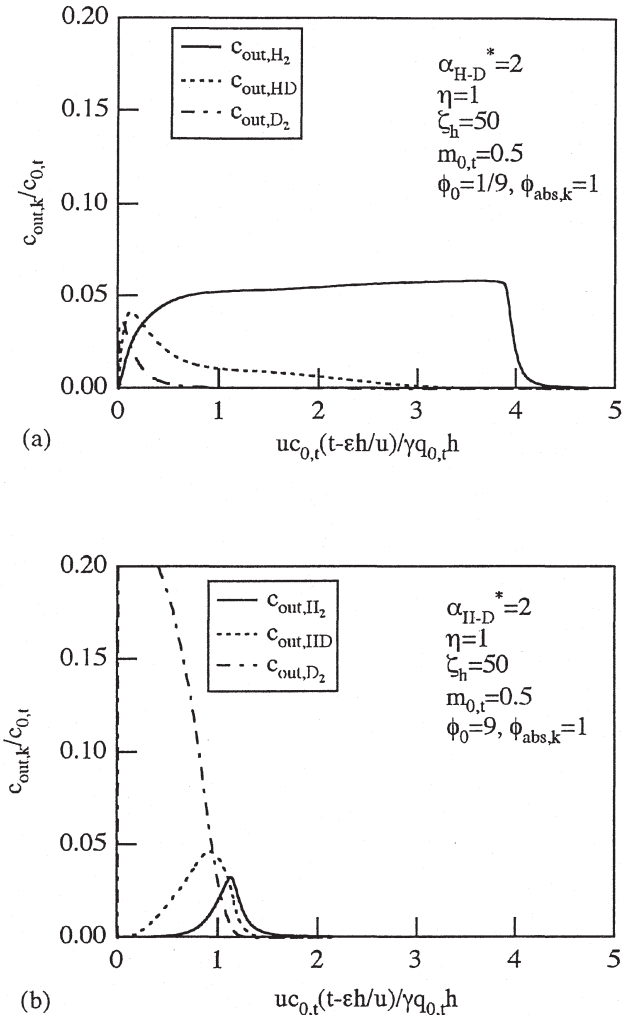

FIG. 9 Variations of hydrogen isotope elution chromatograms with time for different sample concentrations (different ϕ_0 values in the dimensionless form).

der the conditions of low deuterium concentration. In the case of $\phi_0 = 9$, on the other hand, the HD band emerges from the outlet immediately after the sample gas supply. The D_2 purity is not so high that it is difficult to purify the deuterium-dominant sample up to a higher grade. Thus, elution chromatography is efficient only for a gas sample of $\phi_0 \doteqdot 1$.

APPLICATIONS TO FUEL CYCLE SYSTEM

The present simulation is deeply related to a fuel cycle system for an experimental fusion reactor. This is because a mixture of a nearly equal atomic fraction of deuterium and tritium with a small amount of protium is supposed

MARCEL DEKKER, INC.
270 Madison Avenue, New York, New York 10016

to be circulated in the fuel processing loop after removal of other gaseous impurities from the stream. A Pd or Pd alloy particle bed operated at around room temperature is considered the most simplified method for isotope separation.

Here, we consider applications of the Pd bed to an isotope separation system in the fuel cycle of an experimental fusion reactor or in tritium experimental facilities. An equimolar mixture of deuterium and tritium, including a small amount of protium ($c_{H_2,0} + (\frac{1}{2})c_{HD,0})/c_{t,0} = 0.1$ in the molar fraction), is processed by the Pd bed. Other gaseous impurities are removed by a Zr alloy bed from the process lines beforehand. Figure 10 shows a calculation result for the six-component elution chromatography. The elution time is in the order of the T_2, DT, D_2, HT, HD, and H_2 bands. The elution time of the D_2 band is close to those of the HT and HD bands. Therefore, the Pd bed cannot attain complete separation by a once-through operation; i.e., two-step separation is necessary for separation. In the first step a tritium-dominant product continues to be extracted until the D_2 elution time. It includes a trace of protium as HT and HD. When a higher purity of product is demanded, the tritium-dominant gas undergoes the second-step separation process by another Pd bed. The product extracted after the D_2 elution time includes a small amount of tritium and a comparatively large amount of deuterium. In order to raise the deuterium and/or tritium recovery ratio, the protium-dominant gas also undergoes second-step separation action by another Pd bed. Thus, the complete separation of deuterium and tritium from protium can be attained by a recycling operation.

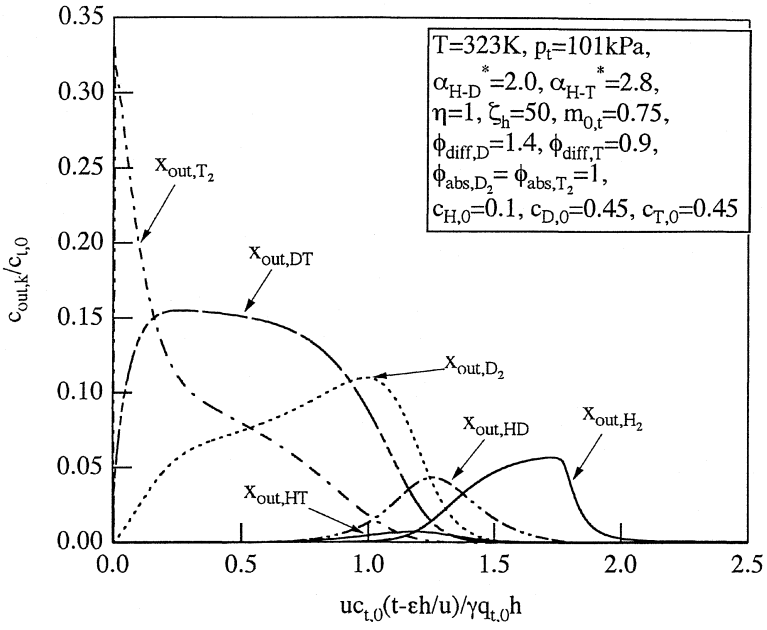

FIG. 10 Elution chromatograms for a six-component hydrogen mixture.

MARCEL DEKKER, INC.
270 Madison Avenue, New York, New York 10016

Although the Pd or Pd alloy bed may not be efficient for continuous and large-scale isotope separation processes in future commercial reactor systems, it surely provides a small-scale, batch operation system for an experimental fusion reactor. The present calculation model may be useful for the prediction of elution chromatograms in such a small-scale, batch isotope separation system.

CONCLUSIONS

An elution chromatography for isotope separation was numerically analyzed in terms of the dimensionless parameters $m_{0,t}$, $\alpha_{H\text{-}D}$, η, ζ_h, ϕ_0, $\phi_{dif,D}$, and $\phi_{abs,k}$. The most affecting parameters among them were especially $m_{0,t}$ and $\alpha_{H\text{-}D}$. This is because the displacement process by the sample gas itself is a key factor. The separation performance is improved with an increase in $\alpha_{H\text{-}D}$ or $m_{0,t}$ within the limitation of each parameter. Judging from many calculations of the elution chromatography, the preferable temperature and $m_{0,t}$ were around 323 K and 0.75, respectively. When a 3-component gas mixture with a ϕ_0 different from unity or a 6-component hydrogen isotope mixture is separated with the Pd bed, it is preferable to operate the process by means of two-step chromatography.

APPENDIX: DIMENSIONLESS GOVERNING EQUATIONS

The dimensionless material balance equation and the dimensionless overall hydrogenation rate equation for each hydrogen species are as follows:

$$\frac{\partial x_k}{\partial \zeta} + \eta\phi_{abs,k}\,(x_k - x_{s,k}) = 0, \qquad k = H_2,\ HD,\ D_2 \tag{A-1}$$

$$\frac{\partial y_{m,j}}{\partial \tau} - \phi_{dif,j}\,(y_{s,j} - y_{m,j}) = 0, \qquad j = H,\ D \tag{A-2}$$

$$y_{s,H} - y_{m,H} = 2\eta\,(x_{H_2} - x_{s,H_2}) + \eta\phi_{abs,HD}\,(x_{HD} - x_{s,HD}) \tag{A-3}$$

$$\phi_{dif,D}\,(y_{s,D} - y_{m,D}) = 2\eta\phi_{abs,D_2}\,(x_{D_2} - x_{s,D_2}) + \eta\phi_{abs,HD}(x_{HD} - x_{s,HD}) \tag{A-4}$$

The dimensionless equilibrium isotherm for each species is as follows:

$$x_{s,H_2} = \left(\frac{y_{s,H}}{y_{s,t}}\right)^2 \frac{c^*_{H_2}(q_{0,t}y_{s,t})}{c_{0,t}} \tag{A-5}$$

$$x_{s,D_2} = \left(\frac{y_{s,D}}{y_{s,t}}\right)^2 \frac{c^*_{D_2}(q_{0,t}y_{s,t})}{c_{0,t}} \tag{A-6}$$

$$x_{s,HD} = (K_{H\text{-}D}x_{s,H_2}x_{s,D_2})^{0.5} \tag{A-7}$$

MARCEL DEKKER, INC.
270 Madison Avenue, New York, New York 10016

$$y_{s,t} = y_{s,H} + y_{s,D} \tag{A-8}$$

After substitution of $c_{s,H_2} = c_{0,H_2}$, $c_{s,D_2} = c_{0,D_2}$, $q_{s,H} = q_{0,H}$, $q_{s,D} = q_{0,D}$, and $q_{s,t} = q_{0,t}$ as the inlet conditions into Eqs. (8) and (12) and some modification using Eq. (25), one obtains an equation to determine $q_{0,t}$ from the data of $c^*_{H_2}$ and $\alpha^*_{H\text{-}D}$:

$$c^*_{H_2}(q_{0,t}) = c_{0,H_2}\left(1 + \frac{\sqrt{\phi^+_{0,D_2}}}{\alpha^*_{H\text{-}D}}\right) \tag{A-9}$$

NOMENCLATURE

a		particle radius (m)
a_v		specific surface area (m^2/m^3)
c_k	$k = H_2$, HD, D_2	hydrogen concentration in gaseous phase (mol/m^3)
$c_{s,k}$	$k = H_2$, HD, D_2	hydrogen surface concentration (mol/m^3)
$c_{0,k}$	$k = H_2$, HD, D_2	inlet hydrogen concentration (mol/m^3)
$c^*_{H_2}(q_{s,t})$		molar density of pure hydrogen in equilibrium with $q_{s,t}$ (mol/m^3)
D_L		axial dispersion coefficient (m^2/s)
$D_{s,j}$	j = H, D	solid phase diffusion coefficient (m^2/s)
h		bed height (m)
j_k	$k = H_2$, HD, D_2	mass flux onto metallic particle per unit volume ($mol/m^2 \cdot s$)
$K_{H\text{-}D}$		equilibrium constant of isotopic exchange reaction (—)
$k_{abs,k}a_v$	$k = H_2$, HD, D_2	absorption rate constant (1/s)
$k_{dif,j}a_v$	j = H, D	solid-phase mass-transfer capacity coefficient (1/s)
$m_{0,t} = ut_0c_{0,t}/\gamma hq_{0,t}$		dimensionless sample amount (—)
p_{H_2}		hydrogen pressure (Pa)
p_t		total pressure (Pa)

MARCEL DEKKER, INC.
270 Madison Avenue, New York, New York 10016

p_0		atmospheric pressure = 101.3 kPa (Pa)
$q_{m,j}$	j = H, D	hydrogen concentration averaged over solid particle (H/Pd)
$q_{s,j}$	j = H, D	hydrogen concentration on solid surface (H/Pd)
R_g		gas law constant (J/mol·K)
r		hydrogen to solid ratio (H/Pd)
r_0		lower limit of plateau region (H/Pd)
t		time (s)
t_0		sample injection time (s)
T		temperature (K)
u		superficial velocity
$x_k = c_k/c_{0,t}$	$k = H_2$, HD, D_2	dimensionless gaseous concentration (—)
$x_{s,k} = c_{s,k}/c_{0,t}$	$k = H_2$, HD, D_2	dimensionless surface concentration (—)
$y_{m,j} = q_{m,j}/q_{0,}t$	j = H, D	dimensionless solid-phase concentration (—)
$y_{s,j} = q_{s,j}/q_{0,t}$	j = H, D	dimensionless surface concentration (—)
z		distance from inlet (m)
$\alpha_{H\text{-}D}$		isotope separation factor between protium and deuterium (—)
$\alpha_{H_2\text{-}HD}$		isotope separation factor between H_2 and HD (—)
$\alpha_{HD\text{-}D_2}$		isotope separation factor between HD and D_2 (—)
γ		molar density of packed bed (mol/m^3)
ε		void ratio (—)
$\phi_{abs,k} = k_{abs,k}/k_{abs,H_2}$		kinetic isotope effect in absorption rate constant (—)
$\phi_{dif,D} = k_{dif,D}/k_{dif,H}$		kinetic isotope effect in hydrogen diffusion in solid particle (—)
$\phi_0 = c_{0,D}/c_{0,H}$		ratio of deuterium to protium concentration at inlet (—)

MARCEL DEKKER, INC.
270 Madison Avenue, New York, New York 10016

$\phi^{+}_{0,k} = c_{0,k}/c_{0,H_2}$	k = HD, D_2	ratio of HD or D_2 to H_2 concentration at inlet (—)
$\Delta\mu^{0}_{H}$		chemical potential difference of hydrogen solution at infinite dilution (J/mol)
ΔH^{excess}_{H}		excess partial molar enthalpy (J/mol)
ΔS^{excess}_{H}		excess partial molar entropy(J/mol·K)
$\eta = \dfrac{c_{0,t} k_{abs,H_2} a_v}{\gamma k_{dif,H}\, a_v q_{0,t}}$		dimensionless mass-transfer parameter (—)
μ^{excess}_{H}		excess chemical potential (J/mol)
$\tau = k_{dif,H} a_v \left(t - \dfrac{\varepsilon z}{u}\right)$		dimensionless time (—)
$\zeta = \dfrac{\gamma k_{diff,H} a_v q_{0,t} z}{u c_{0,t}}$		dimensionless axial distance (—)

Subscripts/Superscripts

0	inlet condition
abs	absorption rate
D	deuterium atom
D_2	D_2 molecule
dif	diffusion in solid particle
excess	excess value
H	protium atom
H_2	H_2 molecule
HD	HD molecule
m	average over particle
plat	plateau
s	surface value
t	total concentration

ACKNOWLEDGMENT

The author is grateful to Prof. Kuniaki Watanabe of Hydrogen Isotope Research Center, Toyama University, for his useful discussion on elution chromatography.

REFERENCES

1. G. Neffe, U. Besserer, J. Dehne, E. Hutter, H. Kissel, R.-D. Penzhorn, J. Wendel, and H. Brunnander, *Fus. Eng. Des.*, *39–40* 987–993 (1997).
2. A. J. P. Martin, *Disc. Faraday Soc.*, *7*, 332 (1949).
3. E. Glueckauf and G. P. Kitt, *Proceedings of the Symposium on Isotope Separation*, *Amsterdam*, 1957 pp. 210–226.
4. F. Botter, J. Menes, S. Tistoschenko, and G. Drianprevious, *Bull. Soc. Chim. Fr.*, *11*, 3374–3382 (1965).
5. F. T. Aldridge, *J. Less-Common Met.*, *108*, 131–150 (1985).
6. S. Fukada, K. Fuchinoue, and M. Nishikawa, *J. Nucl. Sci. Technol.*, *32*, 556–564 (1995).
7. S. Fukada, T. Nakahara, and N. Mitsuishi, *J. Nucl. Mater.*, *171*, 399–407 (1990).
8. N. Mitsuishi, S. Fukada, and N. Tanimura, *J. Less-Common Met.*, *123*, 65–74 (1986).
9. J. C. Giddings, *Dynamics of Chromatography*, Dekker, New York, NY, 1965.
10. E. Kucera, *J. Chromatogr.*, *19*, 237–248 (1965).
11. S. Fukada, H. Matsuo, and N. Mitsuishi, *J. Nucl. Sci. Technol.*, *30*, 171–180 (1993).
12. S. Fukada, T. Yamasaki, H. Matsuo, and N. Mitsuishi, *Ibid.*, *27*, 642–650 (1990).
13. S. Fukada and M. Nishikawa, *Fus. Eng. Des.*, *39–40*, 995–999 (1997).
14. R. Lasser, *Z. Phys. Chem. N. F.*, *143*, 23–49 (1985).
15. K. Watanabe, M. Matsuyama, T. Kobayashi, and W. M. Shu, *Fus. Eng. Des.*, *39–40*, 1001–1008 (1998).
16. T. Kuji, W. A. Oates, B. S. Bowerman, and T. B. Flanagan, *J. Phys. F.*, *13*, 1785–1800 (1983).
17. F. Botter, *J. Less-Common Met.*, *49*, 111–122 (1976).
18. B. M. Andreev, A. D. Polevoi, and A. N. Perevezetsev, *At. Enrgiya*, *45*, 53–58 (1978).
19. J. Volkl, G. Wollenweber, K.-H. Klatt, and G. Alefeld, *Z. Naturforsch.*, *269*, 922–923 (1971).
20. F. Helfferich and G. Klein, *Multicomponent Chromatography*, Dekker, New York, NY, 1970.
21. J. H. Harwell, A. L. Liapis, R. Litchfield, and D. T. Hanson, *Chem. Eng. Sci.*, *35*, 2287–2296 (1980).

Received by editor August 30, 1998
Revision received February 1999

Request Permission or Order Reprints Instantly!